

Modeling of anti-tumor immune response: immunocorrective effect of centimeter electromagnetic waves

O.G. Issaeva^{a,b*} and V.A. Osipov^{a,b}

^a Department of Biophysics, Dubna University, 141980, Dubna, Moscow Region, Russia

^b Bogoliubov Laboratory of Theoretical Physics, Joint Institute for Nuclear Research, 141980, Dubna, Moscow Region, Russia

Abstract

We formulate the dynamical model for the anti-tumor immune response based on intercellular cytokine-mediated interactions with the interleukin-2 (IL-2) taken into account. The production of IL-2 is considered to depend on the antigen presentation. Our study shows that the production rate of IL-2 has a distinct influence on the tumor dynamics. At low production rate of IL-2 a progressive tumor growth takes place to the highest possible value. At high production rate of IL-2 there is a decrease in tumor size to some value when the dynamical equilibrium between the tumor and the immune system is reached. In the case of the medium production rate of IL-2 both these regimes can be realized depending on the initial tumor size and the condition of the immune system. Considering the influence of low-intensity electromagnetic microwaves as a parametric perturbation of the dynamical system, our model predicts a pronounced immunomodulating effect (the suppression of tumor growth and the normalization of IL-2 concentration) which is in good agreement with the recent experimental results on immunocorrective effects of centimeter electromagnetic waves in tumor-bearing mice.

Key words: carcinogenesis, interleukin-2, modeling, anti-tumor immunity, electromagnetic waves.

* Corresponding author. Current address: Bogoliubov Laboratory of Theoretical Physics, Joint Institute for Nuclear Research, 141980, Dubna, Moscow Region, Russia. Fax: (7)(09621) 65084.

E-mail addresses: Issaeva@thsun1.jinr.ru; osipov@thsun1.jinr.ru

1 Introduction

It is well established that the strength of the anti-tumor immune response depends on different cytokines, which play an important role in the development of anti-tumor defence (Alberts, 1994, Roitt, 2000; Wagner et al., 1980). However, any tumor growth results in a disbalance between the production and the regulation of cytokines as well as in a reduction of corresponding receptors. For example, a marked decrease of amounts of interleukin-2 (IL-2) and interleukin-12 (IL-12) during the malignant growth was observed (see, e.g., Berezhnaya and Chekhun, 2000 and the references therein). As a result, the activity of killer cells and, accordingly, the strength of the anti-tumor immune response become weaker (Berezhnaya and Chekhun, 2000).

The methods for enhancement of both the anti-tumor resistance and the general condition of the immune system in tumor-bearing organisms are of current interest. In particular, one of the modern methods in the immunotherapy refers to the use of cytokines (Gause et al., 1996; Hara et al., 1996; Keilholz et al., 1994; Kaempfer et al., 1996). Interleukine-2 is considered as the main cytokine responsible for the proliferation of cells containing IL-2 receptors and their following differentiation (Wagner et al., 1980). IL-2 is mainly produced by activated CD4+ T-cells. IL-2 acts on the same cells that produced it, stimulating their proliferation (autocrine growth). Many investigations give evidence that IL-2 plays an important role in specific immunological reactions to alien agents including tumor cells (Roitt, 2000; Wagner et al., 1980; Liu et al., 2003). Besides, this cytokine provides enhancement of natural killer (NK) cell cytotoxic activity. As is known, NK cells take part in the nonspecific anti-virus and anti-tumor defence. Clinical trials show that there are positive treatment effects at low doses of IL-2 (Hara et al., 1996; Rosenberg and Lotze, 1986; Rosenberg et al., 1994; Schwartzentruber et al., 1993). At the same time, at high doses of IL-2 treatment may cause serious hematologic violations revealed by anemia, granulocytopenia, thrombocytopenia, and lymphocytosis.

Recently, a recovery of IL-2 production after the exposure of tumor-bearing mice to low-intensity centimeter waves was experimentally observed (Glushkova et al., 2003). This indicates that exposure to centimeter electromagnetic waves can be used for an enhancement of the anti-tumor immune response. In experiments, solid tumors were formed by means of hypodermic transplantation of the ascitic Ehrlich's carcinoma cells. This finding stimulates our interest to study the influence of exposure on tumor-immune dynamics.

A theoretical investigation of cancer growth under immunological activity has a long history (see, e.g., Adam and Bellomo, 1996 and the references therein). Most of the known models consider dynamics of two main populations: effector cells and tumor cells. The behavior of cancer growth under the effect of immunity as well as the effect of therapy was the central point of these investigations. The effect of cytokines on the disease dynamics has been considered only in few models. Let us briefly discuss two of them.

The first detailed model for basic players in the anti-tumor immune response including IL-2 was proposed by DeBoer et al. (1985). The main purpose was to study the role of macrophage- T lymphocyte interactions that are involved in the cellular immune response. The model contains eleven ordinary differential equations and five algebraic equations. The analysis of the model shows a possibility for both tumor regression and uncontrolled tumor growth depending on "the degree of antigenicity"

(the initial size of the T lymphocyte precursor populations that can be stimulated upon introduction of specific antigen).

Later, Kirschner and Panetta, (1998) proposed a simpler model where only three populations were considered: the effector cells, the tumor cells, and IL-2. The model allows them to study effects of immunotherapy based on the use of cytokines together with adoptive cellular immunotherapy (ACI). ACI refers to the injection of cultured immune cells that have anti-tumor reactivity into tumor bearing host (Kirschner and Panetta, 1998). Without taking immunotherapy into account they show inability of the immune system to clear the tumor with low antigenicity (a measure of how different the tumor is from 'self') and a reduction of highly antigenic tumors to a small dormant tumor. When tumor exhibits average antigenicity, stable limit cycles were observed. This implies that the tumor and the immune system undergo oscillations.

Further, in the framework of the model by Kirschner and Panetta, 1998, Arciero et al. (2004) considered a novel treatment strategy known as small interfering RNA (siRNA) therapy. The model (Arciero et al., 2004) consists of a system of nonlinear, ordinary differential equations describing tumor cells, immune effectors, the immuno-stimulatory and suppressive cytokines IL-2 and TGF- β as well as siRNA. TGF- β suppresses the immune system by inhibiting the activation of effector cells and reducing tumor antigen receptors. It also stimulates tumor growth by promoting angiogenesis. siRNA treatment suppresses TGF- β production by targeting the mRNA that codes for TGF- β , thereby reducing the presence and effect of TGF- β in tumor cells. The model predicts conditions under which siRNA treatment can be successful in returning TGF- β producing tumors to tumors, producing little or no TGF- β , i.e. non-immune evading state.

The aim of our paper is twofold. First of all, we formulate a mathematical model of anti-tumor immune response with the interleukin-2 taken into account (Sect. 2). To this end, we follow the scheme of intercellular cytokine mediated interaction in cellular immune response proposed by Wagner et al., (1980) which was modified by taking into account co-stimulatory factors such as B7/CD28 and CD40/CD40L instead of interleukin-1 (see, e.g., Liu et al., 2003; Roitt, 2000). As was found, in the absence of these co-stimulatory factors, the presentation of antigen can lead to anergy. This mechanism is potentially responsible for the induction of tolerance to self-antigens. In the framework of the proposed model we study the influence of IL-2 production on the immune response (Sect. 3). And secondly, in Sect. 4 we discuss a possibility of immunomodulating effect within our model and compare it with the available experimental data considering the influence of exposure to electromagnetic microwaves as a parametric perturbation of the initial dynamical system.

2 Model

We will describe the dynamics of cellular populations participating in formation of cytotoxic effector cells and cytokines mediating these reactions in accordance with a scheme presented in Fig.1. Immune response is developed in reply to an appearance of the antigen (AG) in the peripheral lymphoid organs. In the corresponding lymph node, a sufficiently large number of T-cells and B-cells is concentrated which carry specific for a given AG receptors. This provides a high-grade development of immune response in the limited territory.

In order to stimulate development of CD4+ (helper) T cells as well as CD8+ (cytotoxic) T cells specific to tumor antigen (AG), this antigen must be presented via MHC (major histocompatibility complex, in human being — HLA human lymphocyte antigens) class II as well as MHC class I molecules expressed by professional antigen-presenting cell (APC). There are three main types of professional antigen-presenting cells: dendritic cells, macrophages and B cells. Dendritic cells and, to a lesser degree, macrophages have the broadest range of antigen presentation and are probably the most important APC. Initially they exist as immature forms (immature APC or iAPC). iAPC phagocytose AG and degrade its proteins into small pieces and upon maturation present those fragments at their plasma membrane using MHC molecules. Simultaneously, they express co-stimulatory molecules such as B7 and CD40. (Liu et al., 2003; Roitt, 2000). Thus iAPC turn mature APC (mAPC) expressing both complexes AG-MHC-I and II as well as co-stimulatory molecules which are recognized by specific receptors on T cells.

First of all let us formulate the dynamical equations for immature APC (m) and mature APC (M):

$$\dot{m} = V_m - \beta_m m - \gamma_m mg, \quad (1)$$

$$\dot{M} = \gamma_m mg - \beta_M M, \quad (2)$$

In (1) V_m characterizes a steady inflow of iAPC from monocytes (white blood cells which circulate in the body and, depending on the right signal, can turn into either dendritic cells or macrophages). The monocytes in turn are formed from stem cells in the bone marrow. The second term describes iAPC death rate. The production rate of mAPC in (2) is assumed proportional to concentration of iAPC and AG (g).

At all stages of their differentiation (from lymphocyte-precursors coming in the secondary lymphoid organs from timus to mature T lymphocytes) T-cells contain so-called T-cell receptor (TCR) on their surface. By means of TCR T-cell communicates with tumor peptide presented by MHC molecule on the surface of either mAPC or the tumor cell itself. However, this is still insufficient to activate CTL. Actually, it is necessary to bind one more molecule of CTL, CD8 co-receptor, to MHC molecule of a target cell. Despite the fact that TCR for CTL and HTL are coded by identical genes, the co-receptor for HTL is presented by another protein, CD4. Notice that CD4 interacts with MHC-II while CD8 with MHC-I.

Let mAPC present AG with MHC-II molecule to helper T lymphocyte precursor (HTLP) (see signal 1 in Fig.1.) in the presence of a number of co-stimulatory molecules CD40 (signal 2). Molecules CD40 act by force of binding to CD40L markers expressed mainly on helper T cells. In response to these signals activated HTLP produces lymphokines (including IL-2) and corresponding receptors. The similar production is observed when mAPC presents antigen with MHC-I molecule to CTL precursor in the presence of co-stimulatory molecules B7 binding to CD28 markers. The interaction between IL-2 and corresponding receptors on activated T lymphocyte precursors (HTLP and CTL) induces their proliferation and differentiation into mature T lymphocytes (HTL and CTL). At the same time, there is a reason to suppose (Lu et al., 2002; Mizel et al, 1982; Unanue, 1984) that the proliferation of HTL in response solely to IL-2 is absent (or strongly restricted) because the levels of expression of IL-2 receptors on HTL are substantially lower than those observed on CTL (Lu et al., 2002). Hence, to support HTL proliferation the new AG stimulation is required.

In view of the fact that HTL proliferation is restricted, to simplify the model we will not consider a transition of HTL precursors into activated HTL (which produce IL-2 and contain receptors for this cytokine) as well as the proliferation of HTL elicited by

an interaction between IL-2 and corresponding receptors on their surface. Therefore we suggest that the concentration of IL-2 grows linearly with HTLP, APC carrying on their surface AG.

It should be noted that production of IL-2 by HTL decreases at large tumor size. This phenomenon was observed at late stages of the disease (III-IV) while no reliable changes at earlier stages (I-II) of tumor growth were established (see, e.g., Berezhnaya and Chekhun, 2000). It was found that the inhibition of IL-2 results from an accumulation of immuno-suppressing substances, prostaglandines, which both suppress the production of IL-2 and directly destroy its molecules (Liu et al., 2003). Thus, the resulting equations for HTLP (h) and interleukin-2 (I_2) take the form

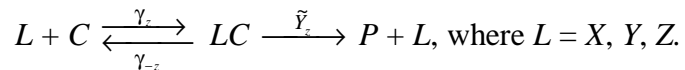
$$\dot{h} = V_h - \beta_h h, \quad (3)$$

$$\dot{I}_2 = \gamma_h hM - \alpha_y yI_2 - \alpha_z zI_2 - \gamma_c cI_2, \quad (4)$$

where V_h characterizes the inflow of HTLP from stem cells. It is suggested that target cells effectively consume IL-2 because IL-2 is a short-distance cytokine. For this reason, we neglect the term presenting loss rate of IL-2.

As was stated above, IL-2-induced proliferation of lymphocytes occurs only after their preliminary stimulation by AG and co-stimulatory factor. At the same time, in accordance with (Smith and Russetty, 1981) a similar (growing) effect of IL-2 can take place with respect to other cells, in particular to CTLP and resting T cells producing a sufficient number of high affinity receptors to IL-2. Therefore we suggest that CTL precursors (the initial production of their high affinity receptors to IL-2 is negligibly small) being stimulated by AG become able to produce a sufficient number of high affinity receptors for IL-2 to activate their proliferation, i.e. they become activated CTLP. For simplicity, let us suppose that activated CTLP transform into a population of proliferating CTL and mature CTL upon contact with IL-2.

Finally, let us formulate the dynamical equations for CTL precursors (x), activated CTLP (y), proliferating CTL and mature CTL (z), tumor cells (c), and tumor-associated antigen (g). In addition, we will introduce an equation for “substratum-enzyme complex”, (lc), suggesting that CTL-tumor cell interaction follows enzymatic kinetics (Merril, 1982; Ochab-Marcinek and Gudowska-Nowak, 2004), that is



Indeed, CTL can be bound to tumor cell either reversibly (direct and reverse reactions with the corresponding rates γ_z and γ_{-z} , tumor cells are not ‘suffering’) or irreversibly (LC complex representing bound cells is formed at the rate proportional to γ_z) inducing cell death (Alberts et al., 1994; Roitt et al., 2000). CTL realize tumor cell killing through one of two main mechanisms. The first one is through the secretion of perforines. Perforines are embedded into a membrane of tumor cell and form pores. As a result, the tumor cell is open for penetrating water. LC complex dissociates into ‘doomed’ tumor cell (P) and CTL (L). Tumor cell swells and gets killed while CTL looks for the new target. The second one is by inducing programmed cell death (apoptosis) through the Fas/Fas ligand pathway. Thus, the last set of equations reads

$$\dot{x} = V_x - \beta_x x - \gamma_x xM - \gamma_z xC + \gamma_{-z}(xC) + \tilde{\gamma}_z(xC), \quad (5)$$

$$\dot{y} = \gamma_x x M - \alpha_y I_2 y - \beta_y y - \gamma_z y c + \gamma_{-z} (y c) + \tilde{\gamma}_z (y c), \quad (6)$$

$$\dot{z} = \alpha_y y I_2 + \alpha_z z I_2 - \beta_z z - \gamma_z z c + \gamma_{-z} (z c) + \tilde{\gamma}_z (z c) \quad (7)$$

$$\dot{c} = -\alpha_c c \ln \frac{\beta_c c}{\alpha_c} - \gamma_z c (x + y + z) + \gamma_{-z} ((x c) + (y c) + (z c)), \quad (8)$$

$$\dot{g} = \alpha_g c - \beta_g g - \gamma_m m g, \quad (9)$$

$$\dot{(lc)} = \gamma_z lc - \gamma_{-z} (lc) - \tilde{\gamma}_z (lc), \text{ где } l = x, y, z. \quad (10)$$

Since the tumor cells grow in conditions of an interior competition one has to use the limiting growth laws such as logistic or Gompertzian. We prefer to choose the Gompertzian law to describe tumor growth (the first term in (8)) because Vladar and Gonzales (2004) have recently shown that the use of the Gompertzian law for tumor growth allows to avoid the regime of tumor autoregression contradicting numerous clinical experiments. It should be noted that in some previous studies either exponential (Garay and Lefever, 1978, Stepanova, 1980; Sherrat and Nowak, 1992) or a logistic growth (Kuznetsov et al., 1994; Kirschner and Panetta, 1998) was explored.

Finally, equations (1)–(10) describe dynamics of cell populations responsible for the anti-tumor immune response. This model allows us to study the different regimes of tumoral growth and immunological activity. However, the formulated model consists of ten differential equations and a great number of model parameters. This makes it difficult to analyze even qualitatively. Therefore, trying to decrease the number of the model equations we will make some simplifying assumptions.

1. First of all let us try to combine all killer T cells into the total population. Indeed, CTL precursors, proliferating CTL, and mature CTL carry both TCR and CD8-co-receptor on their surface. Hence all these cells can be used in the reaction CTL-tumor cells. For lingering diseases one can consider $(lc)(t)$ with $l = x, y, z$ as the rapid variables. In other words, they rapidly reach their stationary values which remain fixed during the time of the immune response. In this case, $\dot{(lc)} = 0$ and one obtains from (10) that $\overline{(lc)} = \gamma_z lc / (\tilde{\gamma}_z + \gamma_{-z})$ with $l = x, y, z$. Substituting this expression in (5)–(8) and summarizing equations (5)–(7) one finally gets

$$\dot{x} + \dot{y} + \dot{z} = V_x + \alpha_z z I_2 - (\beta_x x + \beta_y y + \beta_z z), \quad (11)$$

$$\dot{c} = -\alpha_c c \ln \frac{\beta_c c}{\alpha_c} - \frac{\gamma_z \tilde{\gamma}_z (x + y + z) c}{\gamma_{-z} + \gamma_z}. \quad (12)$$

Here (11) describes a combined population of killer T cells. For convenience, let us mark this population as e (effectors), so that $e = x + y + z$. As the next step, let us take into account the fact that the lifetime of CTL is much shorter in comparison with CTL precursors and activated CTL ($\beta_z \gg \beta_x, \beta_y$). As a result, the equations (11) for killer T cell population presented mainly by CTL that are able to react to corresponding tumor cells (i.e. $e \approx z$) and (12) are reduced to the form

$$\dot{e} = V_x + \alpha_z e I_2 - \beta_z e, \quad (13)$$

$$\dot{c} = -\alpha_c c \ln \frac{\beta_c c}{\alpha_c} - \frac{\gamma_z \tilde{\gamma}_z e c}{\gamma_{-z} + \gamma_z}. \quad (14)$$

Notice that equation (4) for IL-2 is now written as

$$\dot{I}_2 = \gamma_h h M - \tilde{\alpha}_z e I_2 - \gamma_c c I_2. \quad (15)$$

2. Let us assume that $m(t)$, $M(t)$, and $h(t)$ are also rapid variables which reach their constant values \bar{m} , \bar{M} , and \bar{h} , respectively. In this case,

$$V_h - \beta_h h = 0, \quad (16)$$

and, as a result,

$$\dot{I}_2 = \frac{\alpha_{I_2} g}{g + K_c} - \tilde{\alpha}_z e I_2 - \gamma_c c I_2, \quad (17)$$

where expressions for $\alpha_{I_2} = \gamma_h V_h V_m / (\beta_h \beta_M)$ and $K_c = \beta_m / \gamma_m$ come from equations $\dot{m} = 0$, $\dot{M} = 0$, and (16).

3. We suppose that the concentration of AG is proportional to that of tumor cells: $g = k_g c$.

As a result, the model becomes much simpler (it contains only three differential equations) but, nevertheless, it incorporates the most important modern concepts of tumor-immune dynamics including the influence of IL-2 dynamics. For convenience, let us replace $c(t)$, $e(t)$, and $I_2(t)$ by $\xi(t)$, $\eta(t)$, and $\zeta(t)$, respectively, and denote system parameters by Latin letters a_i , b_i , c_i where $i = \xi, \eta$ and ζ :

$$\dot{\xi} = -a_\xi \xi \ln \frac{b_\xi \xi}{a_\xi} - c_\xi \xi \eta \quad (18)$$

$$\dot{\eta} = V_\eta + a_\eta \eta \zeta - b_\eta \eta, \quad (19)$$

$$\dot{\zeta} = \frac{a_\zeta \xi}{\xi + K_\xi} - \tilde{a}_\eta \eta \zeta - c_\zeta \zeta \xi, \quad (20)$$

where $K_\xi = \beta_m / (\gamma_m k_g)$. Notice that the first two equations resemble the famous predator-pray model with tumor cells as ‘victims’. As is seen, the growth rate of ‘predators’ (CTL population) depends on the concentration of IL-2. According to (20) IL-2 production is described by hyperbola. At small ξ the growth rate is linear in tumor size while for big tumor ($\xi \gg K_\xi$) it tends to a constant value. This agrees with the observed decrease of IL-2 production at late stages of illness. The last term in (20) reflects an destruction of IL-2 by metabolic products of tumor cell which are proportional to the concentration of tumor cells.

Before we proceed further, let us point out on some differences between our reduced model and the model by Kirschner and Panetta (1998). First of all, for simplicity we do not consider the mechanisms of natural immunological defense presented by activated macrophages and NK cells in (Kirschner and Panetta, 1998). We suppose that NK cells, macrophages, and cytotoxic T lymphocytes (CTL) have different dynamics. Indeed, according to DeBoer et al. (1985) macrophages and CTL have different capacity to attack tumor cells depending on antigenicity. Namely, tumors with a low degree of antigenicity are attacked mainly by macrophages whereas tumors with high degree of antigenicity can be rejected by CTL only. For this reason, one should extend the model by adding of at least two additional differential equations.

Furthermore, we assume that production of IL-2 is proportional to the number of helper T cells activated by tumor antigen. This agrees with the fact that IL-2 is produced mainly by activated helper T cells (CD4⁺ T cells) (Smith and Ruscetti, 1981; Wagner et al., 1980) (75% of cell-producers of IL-2 are CD4⁺ and 15% are CD8⁺). Notice that in (Kirschner and Panetta, 1998) the effector cells play the role of IL-2 producers. In

addition, we take into account in our model the cytotoxic T cells precursors. In accordance to a theory of the clonal selection they are also able to react with alien agents (in our case with tumor cells) having a specific antigen for CTL on their surface. Finally, we use the Gompertzian law to describe tumor growth, as was discussed above.

2.1. Estimation of the model parameters

An important question is the choice of parameters. The used values are given in Table 1. Notice that some values were taken from the current medical literature including the reduplication time for cells in the ascitic Ehrlich carcinoma (namely this type of carcinoma was used in experiments), the lifetime of CTL (Chao et al., 2004; De Boer et al., 2001), and number of tumor cells when the mice are supposed to be able to survive (DeBoer et al., 1985; Dullens et al., 1979). For remaining unknown parameters, we chose values most appropriate for this model, with the goal to quantify their influence on the model behavior.

2.2. Scaling

For convenience, let us introduce dimensionless variables and parameters as follows: $\xi' = \xi/\xi_0$, $\eta' = \eta/\eta_0$, $\zeta' = \zeta/\zeta_0$, and $t' = t/\tau$ where $\xi_0 = 10^7$, $\eta_0 = 4 \cdot 10^8$, $\zeta_0 = 2 \cdot 10^9$, and $\tau = b_\eta^{-1}$. Notice that the time-scale factor τ is chosen on the basis that the mean lifespan of CTL is about three days and the similar time is needed for the proliferation of CTL and IL-2 (Chao et al., 2004).

Equations (18)–(20) take the form

$$\frac{d\xi'}{dt'} = -\frac{a_\xi}{b_\eta} \xi' \ln \frac{b_\xi \xi_0 \xi'}{a_\xi} - \frac{c_\xi}{b_\eta} \eta_0 \xi' \eta', \quad (21)$$

$$\frac{d\eta'}{dt'} = \frac{V_\eta}{\eta_0 b_\eta} + \frac{a_\eta \zeta_0}{b_\eta} \eta' \zeta' - \eta', \quad (22)$$

$$\frac{d\zeta'}{dt'} = \frac{a_\zeta \xi'}{\zeta_0 b_\eta (\xi' + K'_\xi)} - \frac{\tilde{a}_\eta \eta_0}{b_\eta} \eta' \zeta' - \frac{c_\zeta \xi_0}{b_\eta} \zeta' \xi', \quad (23)$$

where $K'_\xi = K_\xi / \xi_0$. Then, dropping prime notation for convenience, one finally obtains the following scaled model

$$\dot{\xi} = -h_1 \xi \ln \frac{h_2 \xi}{h_1} - h_3 \xi \eta, \quad (24)$$

$$\dot{\eta} = h_4 + h_5 \xi \eta - \eta, \quad (25)$$

$$\dot{\zeta} = \frac{h_6 \xi}{\xi + K'_\xi} - h_7 \eta \zeta - h_8 \xi \zeta, \quad (26)$$

where $h_1 = a_\xi/b_\eta$, $h_2 = b_\xi \xi_0/b_\eta$, $h_3 = c_\xi \eta_0/b_\eta$, $h_4 = V_\eta/b_\eta \eta_0$, $h_5 = a_\eta \zeta_0/b_\eta$, $h_6 = a_\zeta/b_\eta \zeta_0$, $h_7 = \tilde{a}_\eta \eta_0/b_\eta$, and $h_8 = c_\zeta \xi_0/b_\eta$.

3 Steady states analysis

Let us start by the performing a steady state analysis of the system (24)–(26) by using isoclines. It is more informative to use the phase plane $\xi\eta$. In this case, the equations for main isoclines read

$$(h_4 - \eta)(\xi + K'_\xi)(h_7\eta + h_8\xi) + h_5h_6\xi\eta = 0, \quad (27)$$

$$\xi = 0, \eta_{\text{ver}} = -\frac{h_1}{h_3} \ln \frac{h_2\xi}{h_1}. \quad (28)$$

The fixed points are situated at the intersections of isoclines (27) and (28). Our analysis shows that the system (24)–(26) has an unstable point $(0, h_4, 0)$ for any choice of parameters. This point lies at the intersection of isoclines (27) and $\xi = 0$.

In reality, tumor cells develope a number of mechanisms to escape recognition and elimination by immune system. There exist some possible explanations of this phenomenon. The most obvious proposition is that tumors are not immunogenic. The probable reason of nonimmunogenicity is insufficient antigen presentation on the surface of tumor cell (Roitt, 2000). If the tumor cells do not possess antigens of MHC-II, an activation of helper T cells will depend on the processing of tumor antigens by APC. Therefore the IL-2 production will also depend on the antigen presentation. In what follows, different outcomes of the immune response will be investigated.

The efficiency of immune reaction is specified by the parameter a_ζ characterizing the production of IL-2 by helper T cells in response to AG and co-stimulatory factors. The value of a_ζ is taken to vary within the limits shown in Table1. A bifurcation diagram for the dimensionless parameter h_6 is presented in Fig.2. As is seen, there are two bifurcation points. Therefore one can distinguish three main dynamical regimes.

Regime I: for $c_\xi = 1.9 \cdot 10^9 \text{ cells}^{-1} \cdot \text{day}^{-1}$ and $0 < a_\zeta < 1.7 \cdot 10^9 \text{ molecules} \cdot \text{day}^{-1}$ (see Table 1 and Fig. 2) one has two fixed points: a saddle point $(0, h_4, 0)$ and an improper node (ξ_3, η_3, ζ_3) at any initial conditions (see Fig. 3). This means that under a deficiency in the production of IL-2, the population of tumor cells escapes from immune response even though the immune system was initially stimulated. The tumor grows and the immune system becomes suppressed. The point $a_\zeta = 1.7 \cdot 10^9 \text{ molecules} \cdot \text{day}^{-1}$ is the bifurcation point.

Regime II: in the region $(1.7 < a_\zeta < 4.26) \cdot 10^9 \text{ molecules} \cdot \text{day}^{-1}$ there appear two additional fixed points (see Fig. 4): a stable spiral (ξ_1, η_1, ζ_1) and an unstable saddle (ξ_2, η_2, ζ_2) . Therefore different regimes can exist depending on the initial conditions. First, a tumor regresses up to a small fixed size, when the dynamical equilibrium between tumor and immune system is reached. In this case, the tumor manifests itself via the exited immune system. The phase curves follow a stable spiral (Fig. 4, point (ξ_1, η_1)). Second regime appears when $\xi(0) < \xi_2$ and the value of $\eta(0)$ is not big enough to arrive at the dynamical equilibrium. In this case, the tumor grows to a maximum size which corresponds to the maximum possible number of tumor cells in organism. The phase curves pass through the stable node (see Fig. 4, point (ξ_3, η_3)). The same behavior is observed for another initial conditions: $\xi(0) > \xi_2$ and the value of $\eta(0)$ is not big enough for the effective immune response.

Regime III: at $a_\zeta = 4.26 \cdot 10^9 \text{ molecules} \cdot \text{day}^{-1}$ the fixed points (ξ_2, η_2, ζ_2) and (ξ_3, η_3, ζ_3) disappear. As a result, in the region $(4.26 < a_\zeta \leq 5) \cdot 10^9 \text{ mole} \cdot \text{day}^{-1}$ there exist two fixed points: a saddle point $(0, h_4, 0)$ and a stable spiral (ξ_1, η_1, ζ_1) (see Fig. 5). In this case, the dynamical equilibrium between the tumor and the immune system is

established. This state does not depend on either the initial tumor size or the condition of the immune system.

Summarizing, our analysis shows that the production of IL-2 has a definite influence on the possible regimes of cancer dynamics.

4 Influence of electromagnetic microwaves

Before we proceed further, let us briefly discuss the recent experiments (Glushkova et al., 2003) where immunocorrective effects of low-intensity centimeter electromagnetic waves on tumor-bearing mice were observed. Four groups of mice were investigated: control mice, tumor-bearing mice (a transplantation of tumor cells was made in the beginning of the experiment), exposed healthy mice, and exposed tumor-bearing mice. The frequency range of electromagnetic waves used in the experiment is 8.15—18 GHz, the average density of energy flow (intensity) is $1 \mu\text{W}/\text{cm}^2$. Mice were exposed to microwaves daily during 20 days. The duration of the exposure was 1.5 hour. After twenty days of tumor growth the number of splenocytes in tumor-bearing mice was found to be four times over the initial value. At the same time, the concentration of IL-2 in the blood serum of tumor-bearing mice decreased by nearly 20%. As was observed, exposure to microwaves leads to enhancement of anti-tumor resistance in tumor-bearing mice despite the fact that the number of splenocytes is markedly reduced (one and a half times) in comparison with that in unexposed tumor-bearing mice (nevertheless this value is high enough compared to control mice). Both the concentration of IL-2 in the serum of tumor-bearing mice and the production of this cytokine were found to be normalized after exposure to microwaves.

We consider the influence of centimeter waves as the parametric perturbation within our model. Namely, we assume that exposure leads to an increase of the model parameters c_ξ and a_ζ . Let us remind that c_ξ represents the destruction rate of tumor cells by CTL and a_ζ characterizes the production of IL-2. Thus, our assumption means that these parameters depend on wavelength (λ) and intensity of the radiation (I), that is $c_\xi = f(\lambda, I)$ and $a_\zeta = g(\lambda, I)$. To describe the fractional character of exposure we suggest that the parameters c_ξ and a_ζ remain time independent and merely increase to the new constant values $c_{\xi\text{exp}}$ and $a_{\zeta\text{exp}}$. It should be noted that amount of change of c_ξ and a_ζ under exposure is unknown from the experiment. We consider it as the fitting parameter, that is the values chosen in Table 1 for $c_{\xi\text{exp}}$ and $a_{\zeta\text{exp}}$ give the best fit to the experimental data (Glushkova et al., 2003). Notice that the interval (0, 6.6) for t' corresponds to 20 days in real time (since $t = b_\eta^{-1}t'$).

Let us consider the case of a medium IL-2 production rate choosing $a_\zeta = 2.4 \cdot 10^9$ molecules·day $^{-1}$. As is found above, in this case the system has four fixed points. A bifurcation analysis shows that the parametric perturbation due to the electromagnetic influence does not alter the topology of phase portrait (see Fig. 6, the region II), i.e. for chosen values of $a_{\zeta\text{exp}}$ and $c_{\xi\text{exp}}$ (see Table 1) the number of fixed points remains the same. However, their coordinates are changed, so that $\xi_{1\text{exp}} < \xi_1$, $\xi_{2\text{exp}} > \xi_2$, and $\xi_{3\text{exp}} < \xi_3$. Fig. 6 shows both $h_{6\text{min}}$ (the bottom curve) and $h_{6\text{max}}$ (the upper curve) as the function of h_3 . As is seen, three parameter regions for a_ζ and c_ξ exist where the steady regime remains unchanged. The dynamical behavior in these regions exactly corresponds to the regimes I, II, and III mentioned in the previous section.

The results of the numerical integration of the system (24)–(26) are shown in Figs. 7–9. As is seen, functions $\xi'(t')$, $\eta'(t')$ and $\zeta'(t')$ have a damped oscillatory behavior. This means that the immune response is strong enough and continuously stimulated by tumor cells. As is seen from Fig. 7, at first stage the tumor cells grow exponentially, probably, in view of an insufficient number of CTL to activate the immune reaction. Simultaneously, the concentration of IL-2 increases (see Fig. 9) since the tumor antigens stimulate its production. Accordingly, the number of CTL also increases due to an activation of their proliferation by IL-2 (see Fig. 8). In the interval $t' \in (2, 6)$ the concentration of IL-2 is found to decrease. Probably, this is due to the fact that a consumption of IL-2 by CTL prevails the production of this cytokine at this stage of the immune response. The number of CTL keeps on growing for $t' \in (2, 4.5)$. At $t' \approx 2.8$ the population of tumor cells starts to decrease. This is a result of their destruction by CTL. For $t' \in (4.5, 8)$ the concentration of IL-2 is not high enough to continue the proliferation of CTL, so that their number decreases insignificantly and, therefore, the number of tumor cells is slightly increased. The tumor cells in turn stimulate the production of IL-2. This process repeats with decreasing amplitude of oscillations. For $t' > 40$ the dynamical equilibrium is established with $\xi'(t')$, $\eta'(t')$ and $\zeta'(t')$ reaching some constant values. It should be noted that at $t' \approx 6.6$ (i.e. after 20 days of tumor growth) the number of CTL is found to increase approximately four times, and the concentration of IL-2 decreases by nearly 20%. These results are in good agreement with the experimental observations in (Glushkova et al., 2003).

Dotted lines in Figs. 7–9 show the functions $\xi'(t')$, $\eta'(t')$ and $\zeta'(t')$ when the influence of electromagnetic waves is taken into account. As is seen, their behavior is similar to the case of unexposed system. However, due to an increased production of IL-2 under the influence of electromagnetic waves the tumor growth is found to be terminated earlier as compared with the case of unexposed system and everywhere $\xi'_{\text{exp}}(t') < \xi'(t')$. It should be noted that after 20 days of electromagnetic influence the number of CTL is smaller and the concentration of IL-2 is higher than their values in unexposed system. These results are also in qualitative agreement with experiments (Glushkova et al., 2003).

5 Conclusion

In this paper we have formulated the mathematical model for the immune response to the malignant growth with the IL-2 taken into account. The production of IL-2 is considered to depend on the antigen presentation, that is the more antigen-MHC-II complexes are presented by APC to helper T cells the more helper cells are activated to produce IL-2. Within the formulated model the influence of the IL-2 production rate on the efficiency of the immune response is investigated. Our study shows that for a low production of IL-2 the tumor is able to escape from the immune response. For high production rate of IL-2 the decrease of the tumor size is found when the equilibrium between the tumor and the immune system is established. In the case of the medium production of IL-2 there exist two regimes of disease depending on both the initial tumor size and the condition of immune system: i) the regression to small tumor when the dynamical equilibrium is established and ii) a progressive tumor growth to the highest possible value.

Simulating the fractional electromagnetic influence on the immune response, we suppose that the exposure has an influence on two model parameters characterizing both

the rate of inactivation of tumor cells by cytotoxic T cells and the production of IL-2. The values of these parameters are proposed to increase and do not change during an interval of time fixed at numerical calculations. In the experiment, the exposure was being made for 20 days. Since one of our goals is comparison of the model results with the experimental observations (Glushkova et al., 2003), the interval $t' \in (0, 6.6)$ is of the main interest. Our study shows that in 20 days of tumor growth the number of CTL is approximately four times the initial number, and the concentration of the IL-2 decreases by nearly 20%. These conclusions are in good agreement with the experimental results (Glushkova et al., 2003). The electromagnetic influence is found to result in decrease in the number of CTL and in slight increase in the concentration of IL-2 after 20 days of the exposure. These results are in qualitative agreement with the experimental observations in (Glushkova et al., 2003).

It should be noted that any additional experimental data would be vital to test our model. For example, from experiments we know both the number of spleenocytes and the concentration of IL-2 in the blood serum of mice only in the beginning and in the end of the exposure. However, it would be interesting to compare our results (shown in Figs. 7-9) with the experiment at other points of time. Notice also that the influence of electromagnetic waves on the production of the tumor necrosis factor (TNF) was investigated in (Glushkova et al., 2003). As is known, TNF is the cytokine which is produced by macrophages in response to IL-2. It induces the apoptosis mechanisms in both damaged and weakened cells as well as in the tumor cells. The experimental results show that the exposure to microwaves leads to the increase in TNF production. It is quite possible that this cytokine is also responsible for the observed enhancement of the immune response. Experimentally the number of spleenocytes in exposed mice is found to be smaller than in unexposed ones (although it is still high enough in comparison to intact mice). In our model, the dynamics of TNF is not considered. At the same time, we have shown that a decrease of CTL after exposure does not influence the effectiveness of the immune response.

References

1. Adam, J.A. and Bellomo, N. 1996. A survey of Models for Tumor-Immune System Dynamics. Birkhäuser, Boston, MA.
2. Alberts, B., Bray, D., Lewis, J., Raff, M., Roberts, K., Watson, J. D. 1994. Molecular biology of the cell (3rd edition). Garland Publishing Inc., New York, 1408pp.
3. Arciero, J.C., Kirschner, D.E., Jackson, T.L. 2004. A mathematical model of tumor-immune evasion and siRNA treatment. *Disc. Cont. Dyn. Syst.-B.* 4(1), 39—58.
4. Berezhnaya, N.M., Chekhun, V.F., 2000. Interleukines system and cancer. DIA, Kiev, 224pp. (in Russian).
5. Carter, R. H., Drebin, J. A., Schtten, S., Perry, L. L., Greene, M. I. 1983. Regulation of the immune response to tumor antigens. IX. In vitro Lyt 1+2- cell proliferative responses to cell bound or subcellular tumor antigen. *J. Immunol.* 130, 997—1002.
6. Chao, D. L., Davenport, M. P., Forrest, S., and Perelson, A.S. 2004. A stochastic model of cytotoxic T cell responses. *Journal of Theoretical Biology.* 228. 227—240.
7. Czitrom, A. A., Sunshine, G. H., Reme, T., Ceredig, R. Glasebrook, A. L., Kelso, A. and McDonald, H. R. 1983. Stimulator cell requirements for allospecific T-cell subsets specialized accessory cells are required to activate helper but not cytolytic T lymphocyte precursors. *J. Immunol.* 130, 546—550.
8. De Boer, R.J., Hogeweg, P., Dullens, F.J., De Weger, R.A., Den Otter, W. 1985. Macrophage T lymphocyte interactions in the anti-tumor immune response: a mathematical model. *J. Immunol.* 134(4), 2748—2758.
9. De Boer, R.J., Oprera, M., Antia, R., Murali-Krishna, K., Ahmed, R., and Perelson, A. S. 2001. Recruitment times, proliferation, and apoptosis rates during the CD8+ T cell Response to lymphocytic choriomeningitis virus. *Journal of Virology.* 75(22). 10663—10669.
10. Dullens, H.F.J., Vennegoer, C., De Weger, R.A., Woutersen, F., Woutersen, R.A. and Den Otter, W. 1979. Comparison of various forms of therapy in two different mouse tumor systems. *Cancer Treat. Rep.* 63, 99—109.
11. Garay, R., Lefever, R., 1978. A kinetic approach to the immunology of cancer: stationary states properties of effector-target cell reactions. *J. Theor. Biol* 73, 417—438.
12. Gause, B.L., Sznol, M., Kopp, W.C., Janik, J.E., Smith II, J.W., Steis, R.G., Urba, W.J., Sharfman, W., Fenton, R.G., Creekmore, S.P., Holmlund, J., Conlon, K.C., VanderMolen, L.A. and Longo, D.L. 1996. Phase I study of subcutaneously administered interleuking-2 in combination with interferon alfa-2a in patients with advanced cancer. *J. of Clin. Oncol.*, 14(8), 2234—2241.
13. Glushkova, O. V., Novoselova, E. G., Sinotova, O. A., Fesenko, E. E. Immunocorrective effects of Ultrahigh-frequency Waves on tumor-bearing mice. 2003. *Biophysics.* 48(2), 281-288.
14. Greene, M.I. 1980. The genetic and cellular basis of regulation of the immune response to tumor antigens. *Contemp. Top. Immunobiol.* 11, 81—116.
15. Hara, I., Hotta, H., Sato, N., Eto, H., Arakava, S. and Kamidono, S. 1996. Rejection of mouse renal cell carcinoma elicited by local secretion of interleukin-2. *J. Cancer Res.*, 87, 724—729.
16. Kaempfer, R., Gerez, L., Farbstein, H., Madar, L., Hirschman, O., Nussinovich R. and Shapiro A. 1996. Prediction of response to treatment in superficial bladder

carcinoma through pattern of interleukin-2 gene expression. *J. of Clin. Oncol.* 14(6), 1778—1786.

17. Keiholz, U., Scheibenbogen, C., Stoelben, E., Saeger, H. D. and Hunstein, W. 1994. Immunotherapy of metastatic melanoma with interferon-alpha and interleukin-2: pattern of progression in responders and patients with stable disease with or without resection of residual lesions. *European J. of Cancer.* 30A(7), 955—958.
18. Kirschner, D., Panetta, J. C. 1998. Modeling immunotherapy of the tumor-immune interaction. *J. of Mathematical Biology.* 37, 235—252.
19. Kuznetsov, V., Makalkin, I., Taylor, M., Perelson, A. 1994 Nonlinear dynamics of immunogenic tumors: parameter estimation and global bifurcation analysis. *Bull. Math. Biol.* 56(2), 295—321.
20. Liu, Y., Ng, Y., and Lillehei, K. O. 2003. Cell mediated immunotherapy: a new approach to the treatment of malignant glioma. *Cancer Control.* 10(2), 138—147.
21. Lu, J., Giuntoli, R. L., II, Omiya, R., Kobayashi, H., Kennedy, R., and Celis, E. 2002. Interleukin 15 promotes antigen-independent in vitro expansion and long-term survival of antitumor cytotoxic T lymphocytes. *Clinical Cancer Research.* 8, 3877—3884.
22. Merrill, S. J. 1982. Foundations of the use of an enzyme-kinetic analogy in cell-mediated cytotoxicity. *Math. Biosci.* 62, 219—235.
23. Mizel, S. B. 1982. Interleukin 1 and T cell activation. *Immunol. Rev.* 63, 51—72.
24. Ochab-Marcinek, A., Gudowska-Nowak, E. 2004. Population growth and control in stochastic models of cancer development. *Physica A* 343, 557-572.
25. Roitt, I., Brostoff, J., Male, D., 2001. *Immunology* (6th edition). Mosby, London, 480pp.
26. Rosenberg, S. A. and Lotze, M. T. 1986. Cancer immunotherapy using interleukin-2 and interleukin-2-activated lymphocytes. *Annual Review of Immunology.* 4, 681—709.
27. Rosenberg, S. A., Yang, J. C., Topalian, S. L., Schwartzentruber, D. J., Weber, J. S., Parkinson, D. R., Seipp, C. A., Einhorn, J. H. and White, D. E. 1994. Treatment of 283 consecutive patients with metastatic melanoma or renal cell cancer using high-dose bolus interleukin 2, *JAMA*, 271(12), 907—913.
28. Schwartzentruber, D. J. 1993. In Vitro predictors of clinical response in patients receiving interleukin-2-based immunotherapy. *Current opinion in oncology.* 5, 1055—1058.
29. Sherratt, J., Nowak, M., 1992. Oncogenes, anti-oncogenes and the immune response to cancer: a mathematical model. *Proc. R. Soc. London B* 248, 261—271.
30. Smith, K. A. and Ruscetti, F. W. 1981. T-cell growth factor and the culture of cloned functional T cells. *Adv. Immunol.* 31, 137—175.
31. Stepanova, N., 1980. Course of the immune reaction during the development of a malignant tumor. *Biophysics* 24, 917—923.
32. Unanue, E. R. 1984. Antigen-presenting function of the macrophage. *Annu. Rev. Immunol.* 2, 395—428.
33. Vladar, H. P. and Gonzalez, J. A., 2004. Dynamic response of cancer under the influence of immunological activity and therapy. *J. Theor. Biol.* 227, 335—348.
doi:10.1016/j.jtbi.2003.11.012
34. Wagner, H., Hardt, C., Heeg, K., Pfizenmaier, K., Solbach, W., Bartlett, R., Stockinger, H. and Rollingoff, M. 1980. T-T cell interactions during CTL responses:

T cell derived helper factor (interleukin 2) as a probe to analyze CTL responsiveness and thymic maturation of CTL progenitors. Immunol. Rev. 51, 215—255.

Figure Captions

Fig. 1. The suggested scheme of the T cell mediated immune response.

Fig. 2. Bifurcation diagram varying h_6 . For $h_6 < 2.62$ there is only one steady state — improper node (I). When $2.62 < h_6 < 6.45$ there are two stable steady states — improper node and spiral node, and an unstable (saddle) point (II). For $h_6 > 6.45$ only one steady state, spiral node remains (III).

Fig. 3. The phase curves in the case of the low IL-2 production rate ($a_\zeta = 1.1 \cdot 10^9$ molecules·day $^{-1}$).

Fig. 4. The phase curves in the case of the medium IL-2 production rate ($a_\zeta = 2.4 \cdot 10^9$ molecules·day $^{-1}$).

Fig. 5. The phase curves in the case of the high IL-2 production rate ($a_\zeta = 5 \cdot 10^9$ molecules·day $^{-1}$).

Fig. 6. A two-parameter bifurcation diagram of IL-2-production versus tumor cells inactivation (a_ζ vs. c_ξ). Each point of the bottom curve is the bifurcation point where two steady states are created, each point of the upper curve is the bifurcation point where two steady states disappear and the only spiral node remains.

Fig. 7. Time dependence of the number of tumor cells (solid line — unexposed system, dotted line — exposed system). The point $t' = 6.6$ ($t \approx 20$ days) is marked on the axis

Fig. 8. Time dependence of the number of CTL (solid line — unexposed system, dotted line — exposed system). The influence of electromagnetic waves on the number of the splenocytes in mice is shown on the experimental diagram in the inset. On the y-axis the number of splenocytes ($\times 10^6$) is shown in: 1 — control mice, 2 — exposed healthy mice, 3 — tumor-bearing mice, 4 — exposed tumor-bearing mice.

Fig. 9. Time dependence of the concentration of IL-2 (solid line — unexposed system, dotted line — exposed system). The inset highlights the concentration of the IL-2 in the serum of mice (light column). On the y-axis the concentration of the IL-2, % of the control concentration is shown in: 1 — exposed mice, 2 — the tumor-bearing mice, 3 — the exposed tumor-bearing mice.

Table 1. The values of the model parameters

(20)	$a_\xi = 0.165 \text{ day}^{-1}$	$b_\xi = 1.6 \cdot 10^{-9} \text{ cells}^{-1} \cdot \text{day}^{-1}$	$c_\xi = 1.9 \cdot 10^{-9} \text{ cells}^{-1} \cdot \text{day}^{-1}$
			$c_{\xi \text{exp}} = 2.2 \cdot 10^{-9} \text{ cells}^{-1} \cdot \text{day}^{-1}$
(21)	$V_\eta = 5.9 \cdot 10^6 \text{ cells} \cdot \text{day}^{-1}$	$a_\eta = 1.5 \cdot 10^{-10} \text{ cells}^{-1} \cdot \text{day}^{-1}$	$b_\eta = 0.33 \text{ day}^{-1}$
	$0 \leq a_\zeta \leq 5 \cdot 10^9 \text{ molecules} \cdot \text{day}^{-1}$		
(22)	$a_{\zeta \text{exp}} = 3 \cdot 10^9 \text{ molecules} \cdot \text{day}^{-1}$	$\tilde{a}_\eta = 1.1 \cdot 10^{-9} \text{ cells}^{-1} \cdot \text{day}^{-1}$	$c_\zeta = 5 \cdot 10^{-8} \text{ cells}^{-1} \cdot \text{day}^{-1}$
	$K_\xi = 1.2 \cdot 10^6 \text{ c.}$		

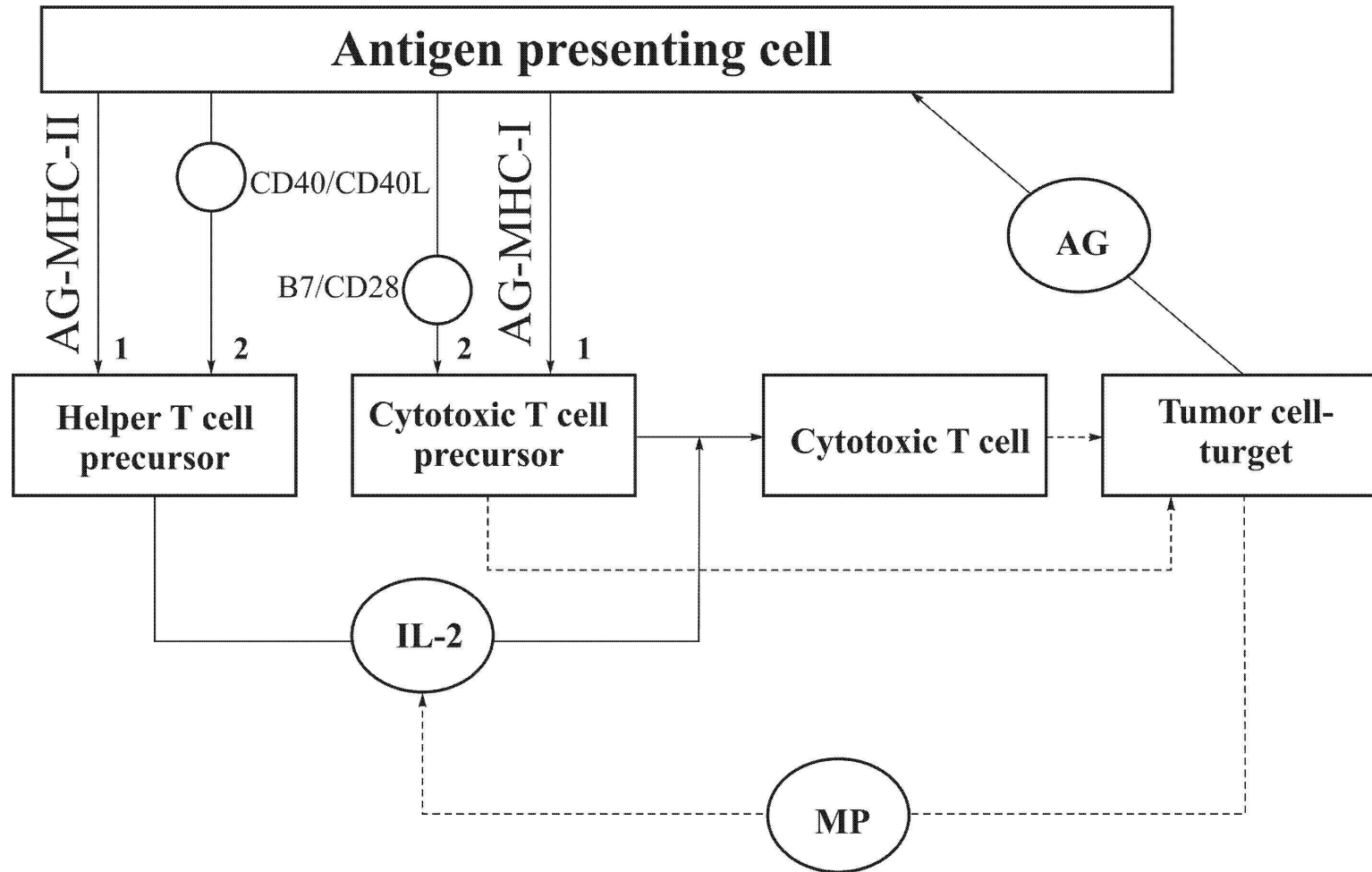


Fig. 1.

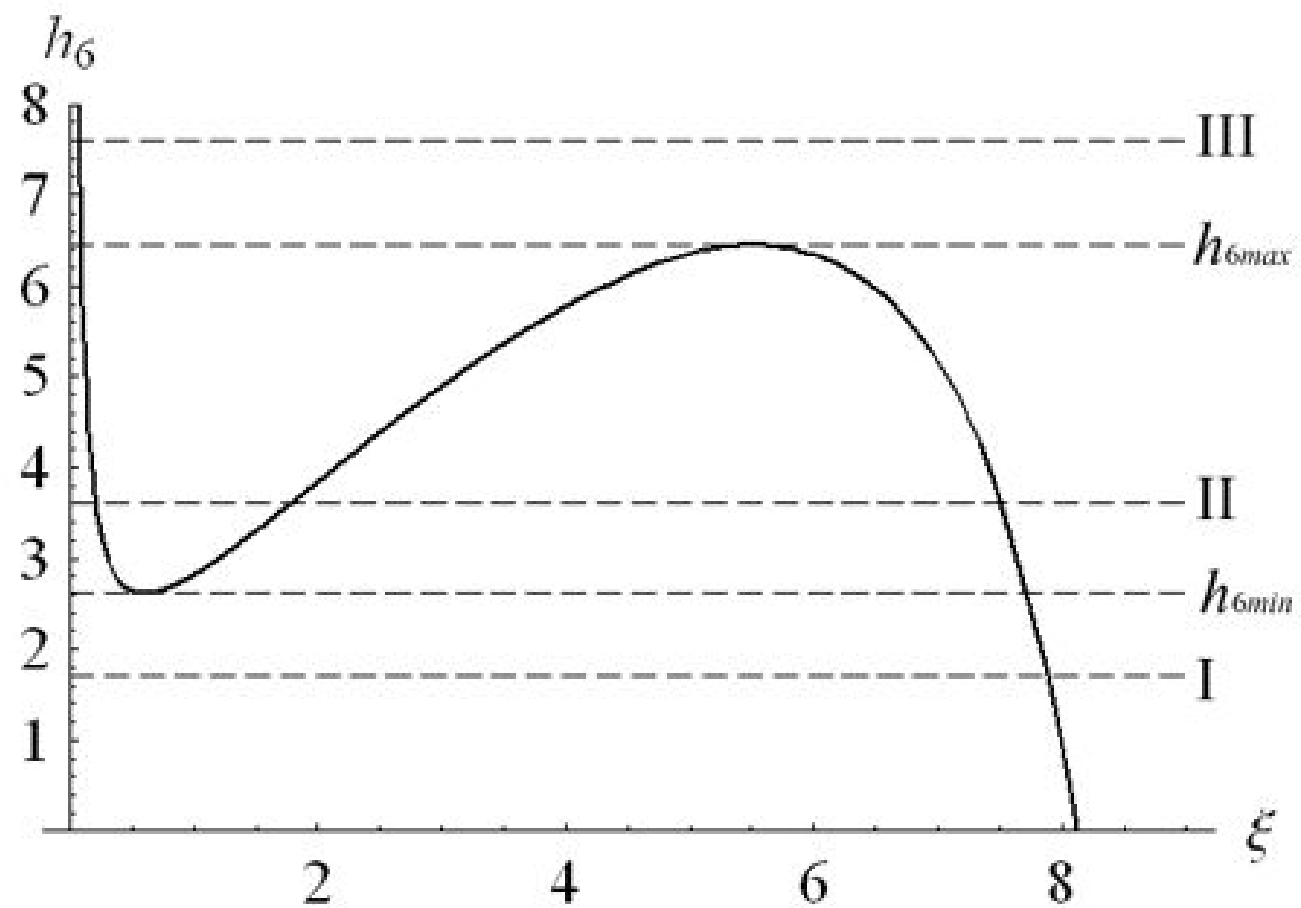


Fig. 2.

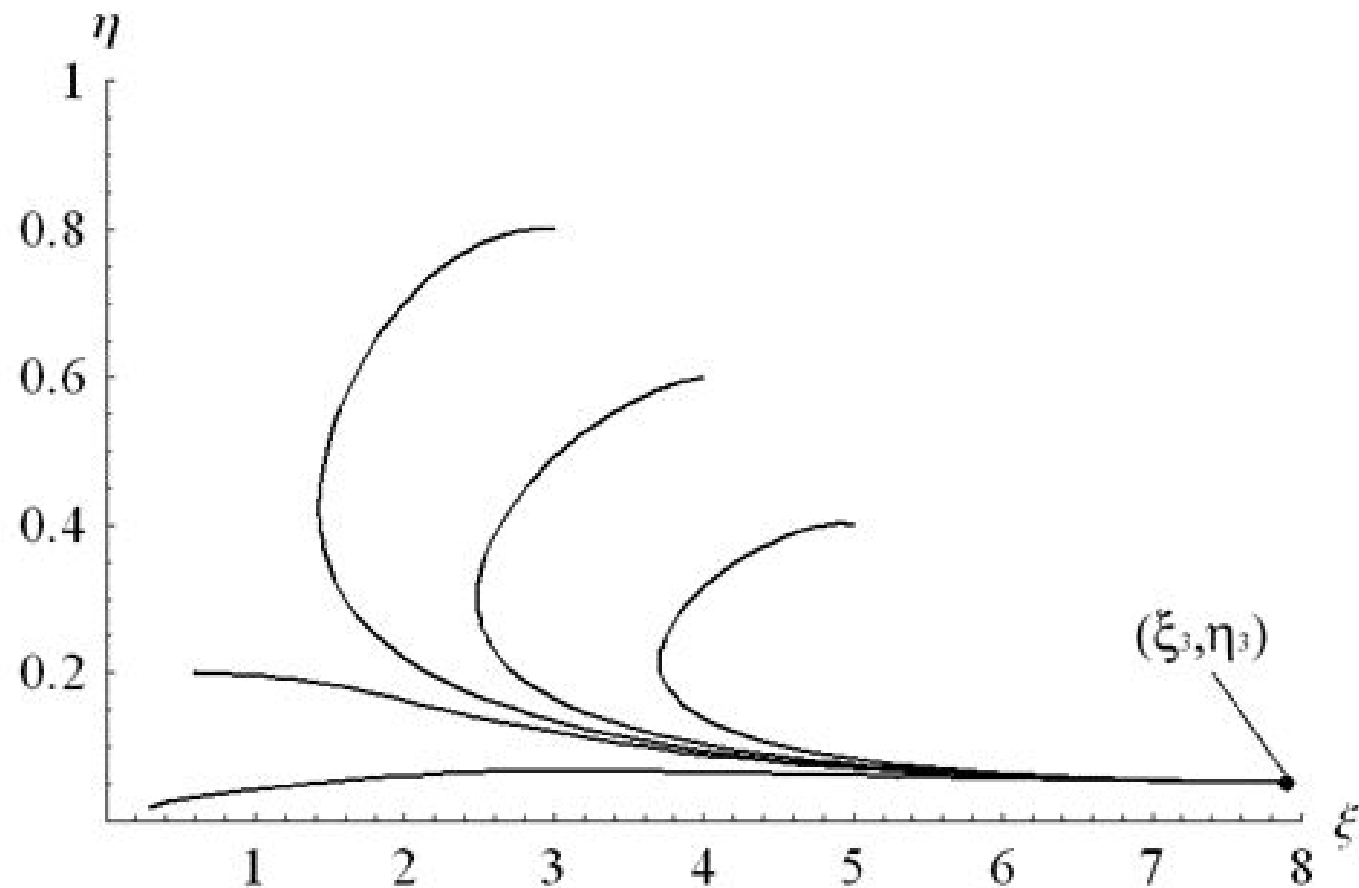


Fig. 3.

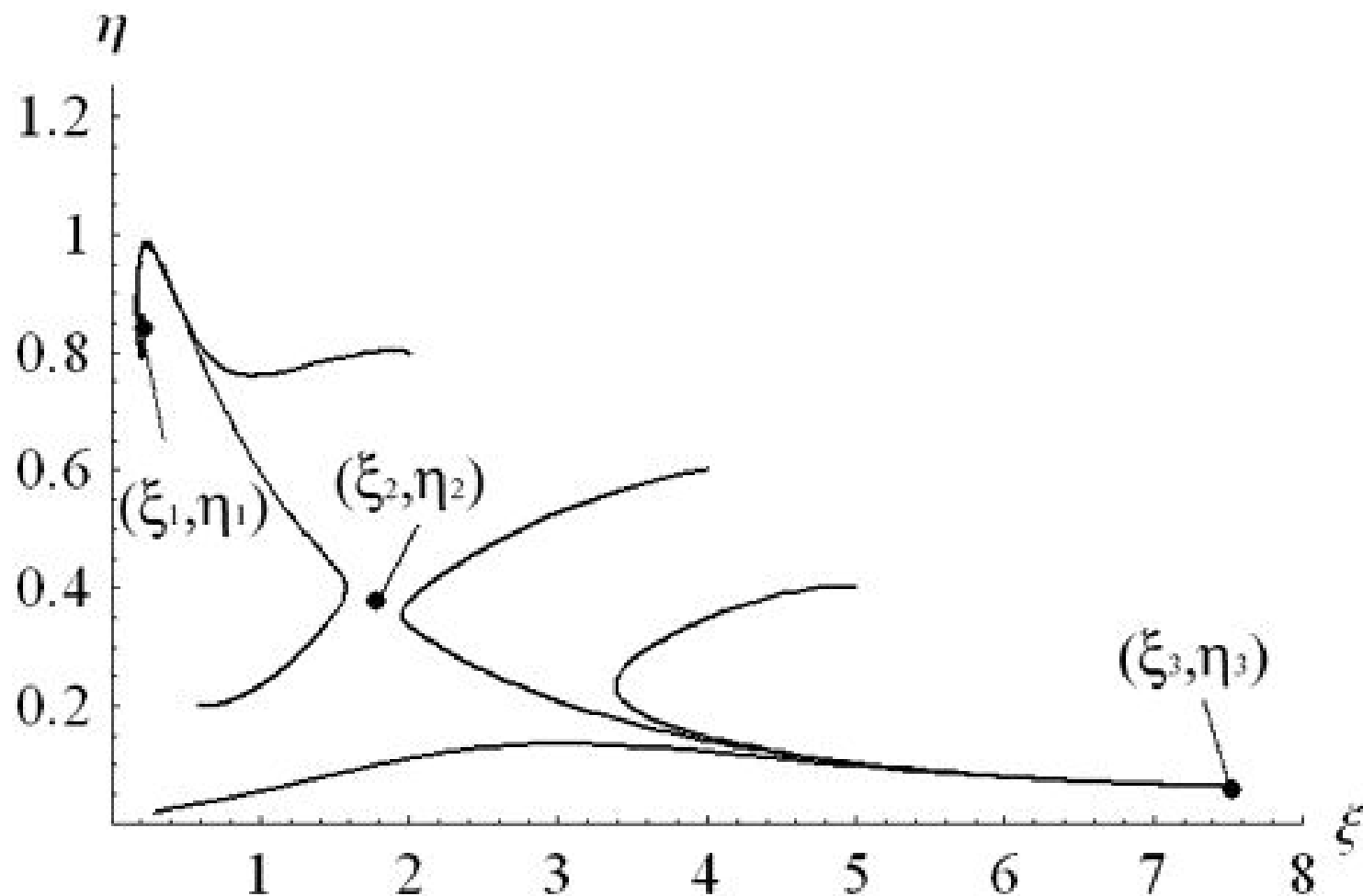


Fig. 4

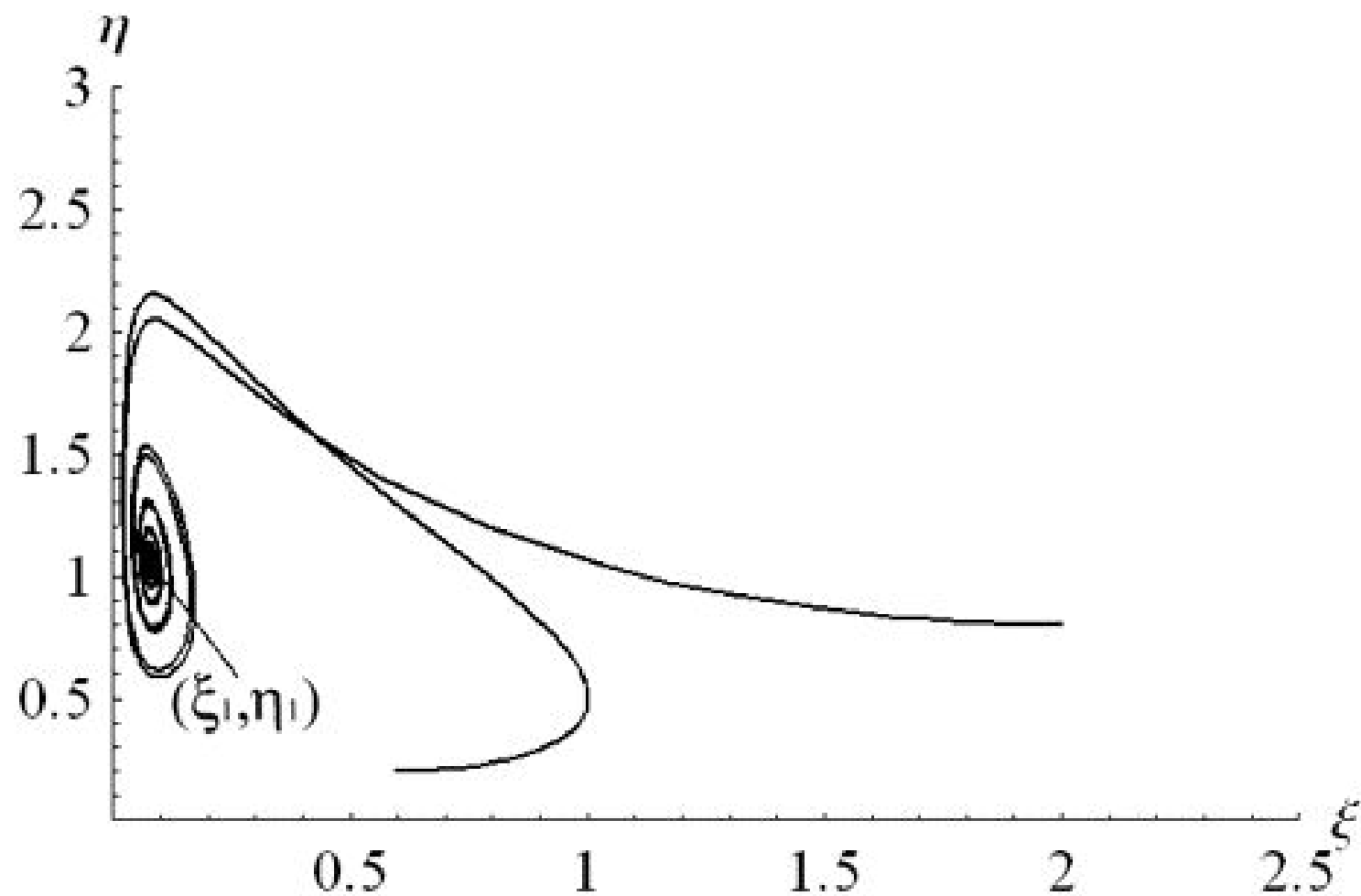


Fig. 5

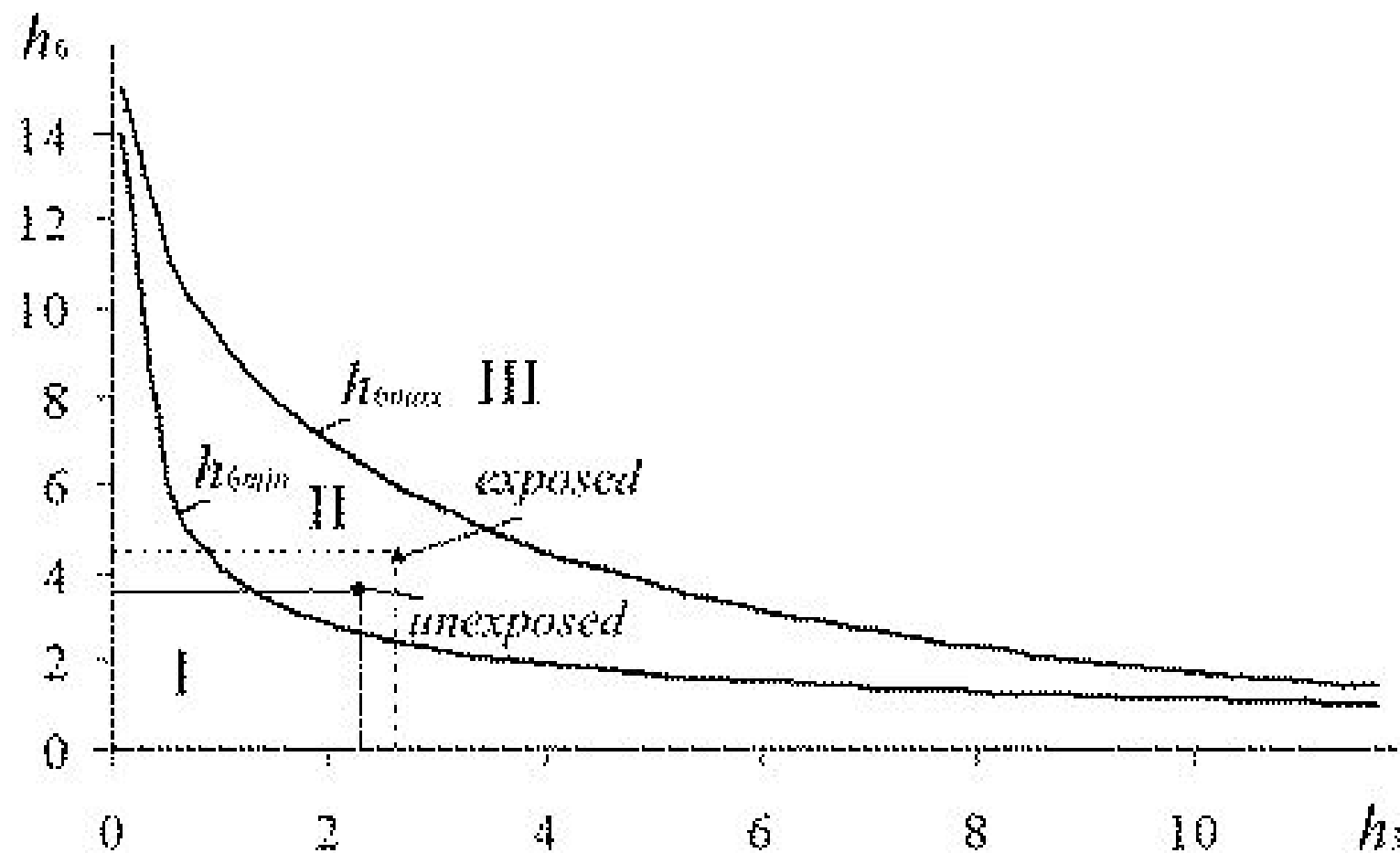


Fig. 6

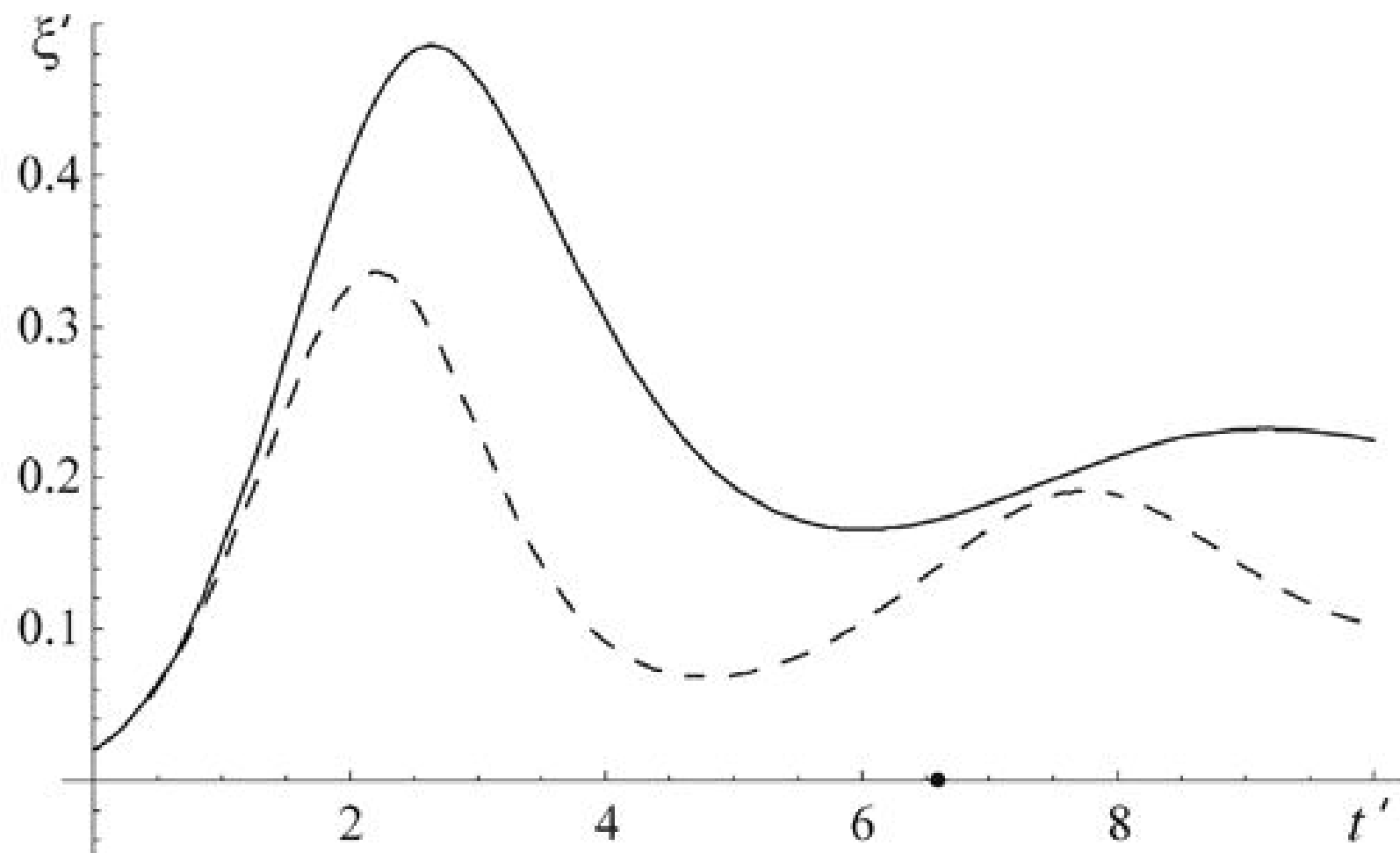


Fig. 7

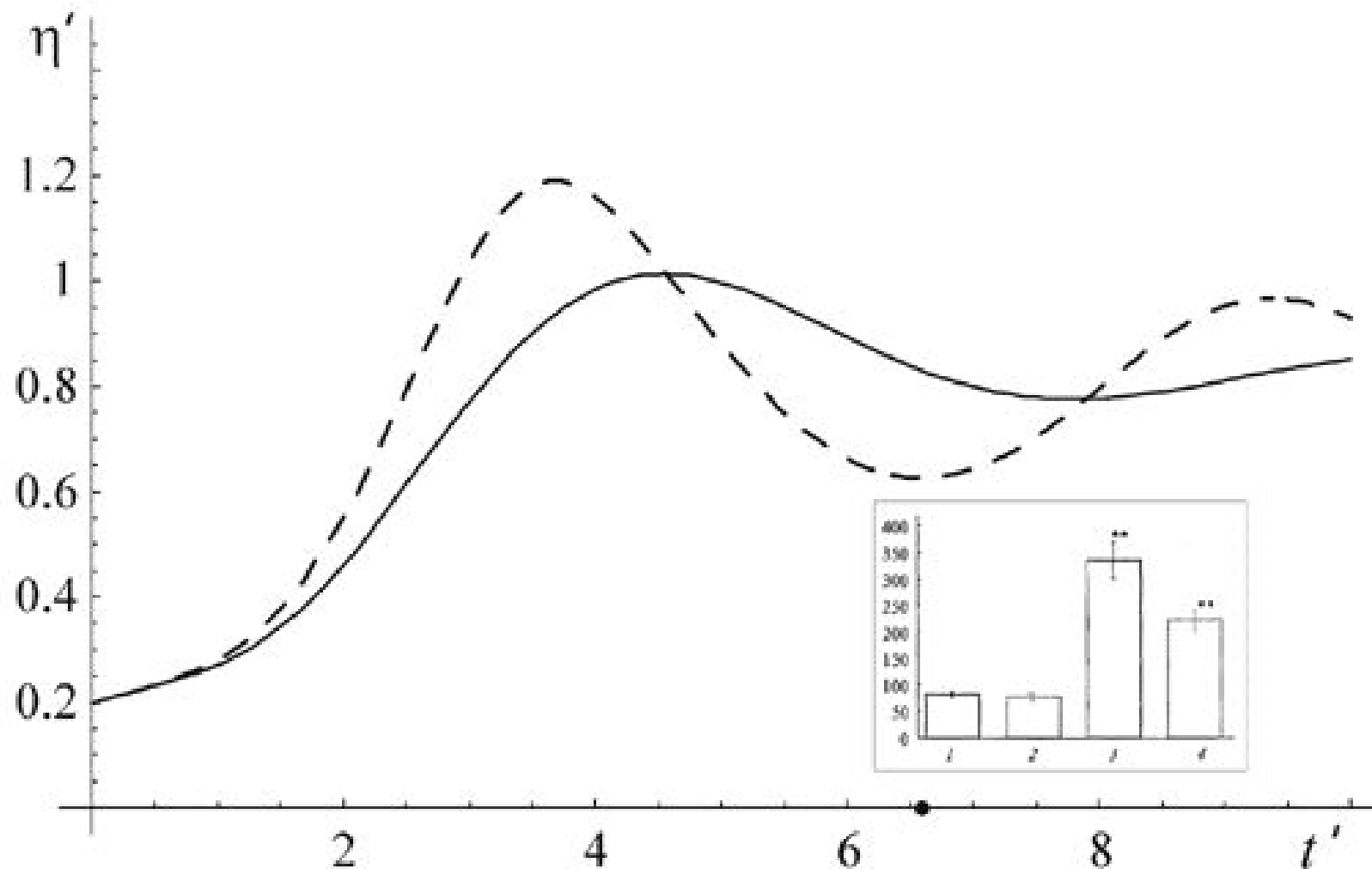


Fig. 8

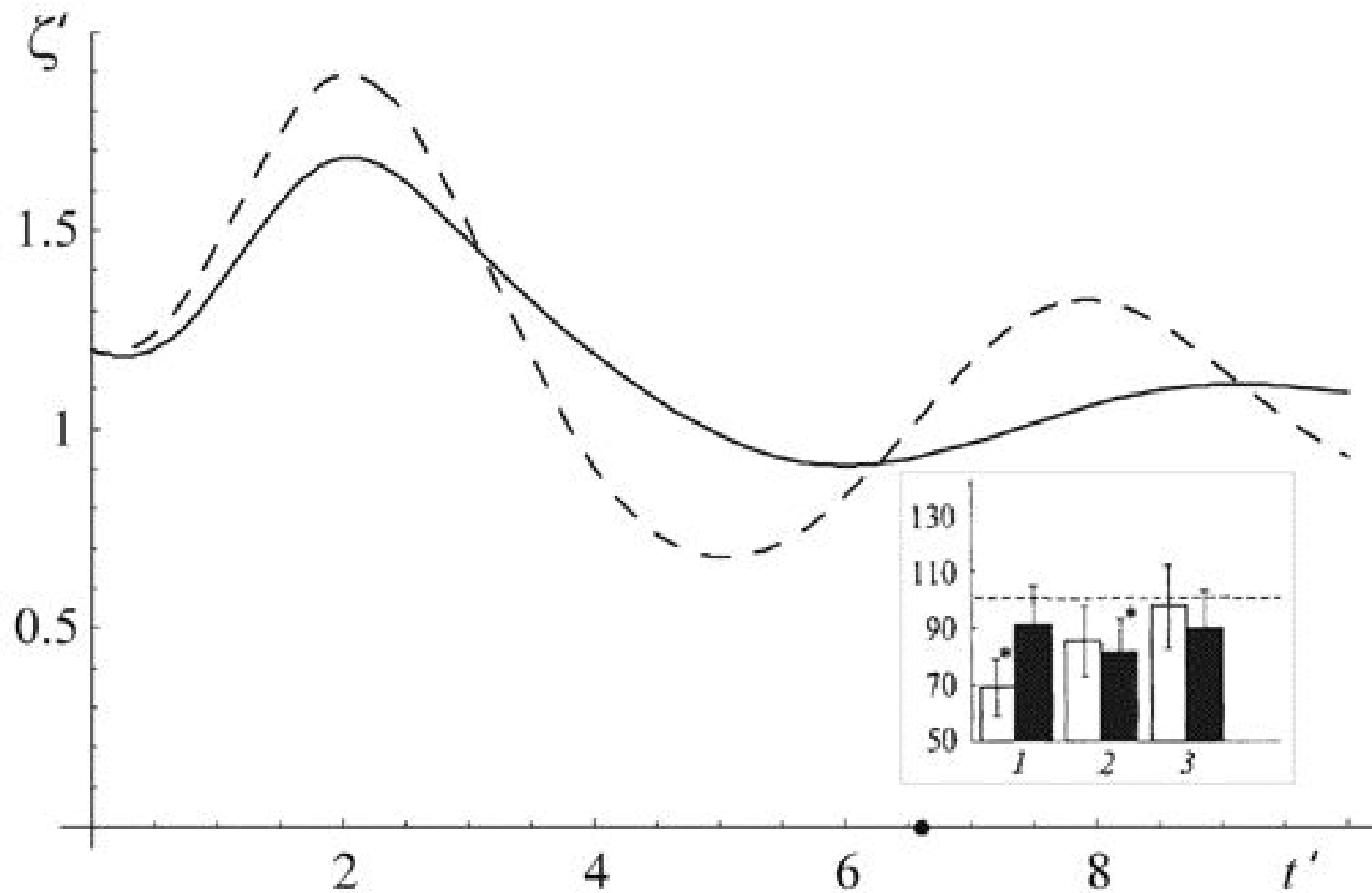


Fig. 9